Leonardo Electronic Journal of Practices and Technologies Issue 16, January-June 2010
ISSN 1583-1078 p. 101-118

Application of Time Delay Consideration on Bridge Vibration Control Method with Active Tendons

Lezin Seba MINSILI[1]* and He XIA[2]

[1] *Sr. Lecturer, IABSE member, LMM Laboratory, Department of Civil Engineering, ENSP, the University of Yaoundé 1, PO. Box 8390 Yaoundé, Cameroon*
[2] *Professor, IABSE member, School of Civil Engineering, Beijing Jiaotong University, 100044 Beijing China*
E-mails: lezinsm@yahoo.com*, hxia88@163.com

(* Corresponding author: Phone: (+237) 7792 2659, Fax: (+237) 2222 4547)

Abstract

For many years bridge structures have been designed or constructed as passive structures that rely on their mass and solidity to resist external forces, while being incapable of adapting to the dynamics of an ever-changing environment. When the rigidity assumption is not met in particular for high-rise structures like bridge towers, a proper dynamic model should be established and conclusions made on the differential vibration of the tower when it is investigated out of the bridge system. The present work outlines a vibration control method by tendons on the tower of cable supported structures considering time delay effects, based on the discrete-time Linearization of the Feedback Gain Matrix. The efficiency of this vibration control method first proposed on the design process of a local bridge in Cameroon, is more compatible to the control of civil structures and is of great interest in accordance with simulation results.

Keywords

Vibration Control; Bridge Tower; Active Tendon; Linearization; Feedback Gain Matrix.

Introduction

Evolution of sustainable human settlements in developing countries and more specifically in Africa requires research that has the dimension of cultures at the heart of an implementation strategy. This position compels local engineers to acquire and use scientific, technical and other pertinent knowledge and skills to create, operate, and maintain efficient systems, machines, plants, processes and devices of practical values. The aim of the present research work is to promote and to foster the appropriation of adequate technical expertise for the local construction industry as a key vital issue if the society must enjoy modern structures like bridges amidst the ever increasing demand of transport utilities. The appropriation of proved scientific expertise in the last five years has been a challenge for the National Civil Engineering Laboratory (LABOGENIE) in acquiring modern test equipments and in improving research facilities for its members in order to facilitate technology transfer between local experts and foreign experts from Asia and Europe

Prestressed tendons in active control system are connected to a structure whose vibrations are controlled and to an electro-hydraulic servomechanisms or actuators with a function to control the tension in the tendon. If a servomechanism is properly and timely regulated, the tendon can operate in the pulsed mode as well as in the continuous time mode. These active tendons have been studied analytically by many authors (Mohamed [1], Deger [2], Achkire [3]) in connection with control of slender structures, tall buildings or bridges. Hiroshi et al [4] presented an experimental effective method to control the first tree modes of a cable-stayed bridge using the active control system. Many tests done on cable-stayed bridges revealed that vibrations induced by stay cables have a significant influence on the motion of the superstructure and have to be considered in data analysis.

Some works [5, 6] were done to control the dynamic vibration of the cables or the decks system of contemporary bridges where the tower was considered as a fixed unmovable structure like a wall. A proper dynamic model should be established and conclusions be made on the differential vibration of the tower when it is investigated out of the bridge system. The dynamic model of a tower depends to a large extent on the effort one wants to put into a theoretical investigation. To reduce such efforts, the cable systems may be replaced by its linear spring stiffness in the plane with or without the cable generalized system mass, and the tower itself may be discretized into lumped or distributed masses. Researches and

developments of active and/or semi-active dampers have been carried out during the past several years because of their high performance and low power demand. Bernd Köberl and Johann Kollegger [6] reported recently a high frequency testing facility, for stay cables and tendons with a testing load up to 20000 kN that can be operational on the tower head or on the bridge desk. And from massive design and construction of cable stayed bridges in China, some under-developed countries in Africa like Cameroon [7] have launched several national projects on infrastructures like dams and bridges.

The purpose of the present work is to outline the application of a vibration control method by tendons on the tower of cable-supported structures considering time delay effects, based on the discrete-time "Linearization of the Feedback Gain Matrix" provided by the same author[8]. In practice, time has to be consumed during data processing, online computation and control force application, thus inevitable time delay in control execution makes it necessary to consider appropriate modifications to the control algorithm in the form of an optimization problem converted to the minimization of the performance index subjected to appropriate constraints. This vibration control method taking into account time delay compensation has been applied to the design process of a local bridge in Cameroon. It is more efficient with comparison to the control of civil structures, and attracts great interest in simulation results obtained through sinusoidal and earthquake inputs. If time-delay is neglected, the control system is susceptible to develop dynamic instability, and therefore, it is better not to apply control actions into a structural system before the time-delay is properly analyzed and tackled.

Material and Method

Description of the Bridge System

Cable supported bridges are competitive for spans in the range from 200m to 2000m (and beyond), thus covering approximately 90% of the present span range [9]. The structural system of cable supported bridges consists of four main components: the stiffening girder (or truss) with the bridge deck, the cable system supporting the stiffening girder, the Towers (or pylons) supporting the cable system, and the anchor blocks (or piers) supporting the cable

system. The anchor blocks (or piers) support the cable system vertically and horizontally or only vertically at the extreme ends. Different types of cable supported bridges are distinctively characterized by the configuration of the cable system. Combined systems containing both suspension system and cable-stayed system have been applied in the cable supported bridges built in the 19th century, most notably in the Brooklyn Bridge having stay cables in the Fan configuration as a supplement to its parabolic main cables and vertical hangars. The same configuration can be found in the combined suspension and cable-stayed bridge between Hong Kong and the inner Ling Ding Island [10].

Figure 1. *A false configuration model of a cable-stayed bridge at the Saint-Anastasie Park in Yaoundé-Cameroon*

In Cameroon, there is still no constructed cable supported bridge, even though one can find in some parks kits of cable stayed footbridge as the one inside the Saint-Anastasie Park in Yaoundé (Figure 1), where a local architect has falsely designed the bridge with its deck supporting the pylon and the cables. Many design offices have recruited qualified structural engineers and have proposed different configurations of cable supported bridges, as they are competing to win the ongoing design BID of the bridge crossing the Wouri River in Douala. The present bridge built in 1954 crosses the Wouri river with sixteen simply-supported pre-stressed concrete (PC) girders of 45 m span and 14.60 m width, and carries one railroad between two single-line roadways, each with a sidewalk [11, 8]. One of the proposed design configuration, though rejected for insufficient technical expertise from the tender, deals with a

combined cable supported bridge. The total length of the projected bridge is 1520m, with a central span of 1040 m and two side spans of 240.0 m as shown in Figure 2.

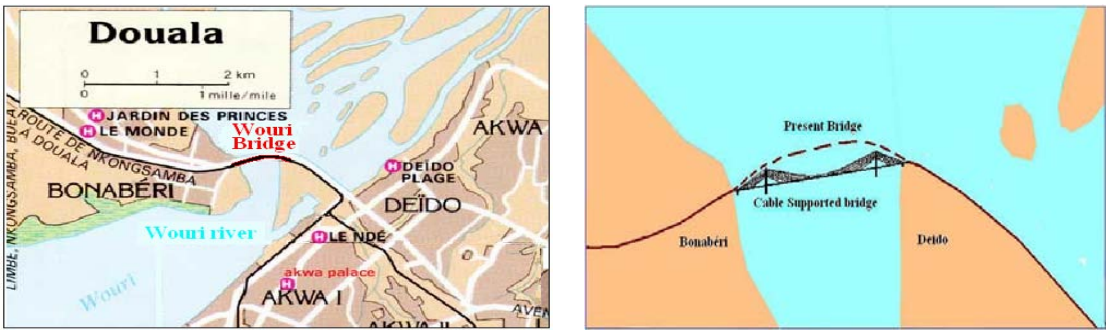

Figure 2. *Present and Projected Bridge locations*

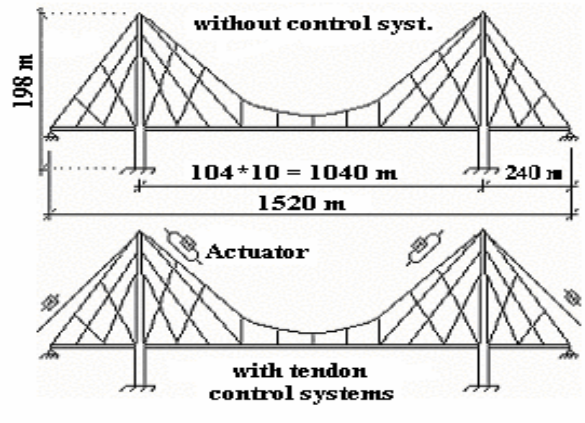

a) 2-D tower model used in this work *b) Actuators anchored in the pylon*

Figure 3. *Pylon and bridge configurations*

The bridge deck has a three cells box section, 3.76 m wide and 4.6 m depth. The upper and lower slabs are 0.300 m thick while the inclined stay-walls are 0.350 m thick. Along its span the box is stiffened by a set of transversal beams, placed in correspondence to the stay-cables. The two pylons of the cable-supported bridge are 198.0 m high from the floor level and are assembled from two rectangular hollow sections constituting a framed tower as shown in Figure 3. The section of the tower and related characteristics varies with its height. Each side of the pylon carries the devices used to anchor the stay-cables and the control cables leaving them, crossed but not intersected on the same plane. To satisfy the future navigation requirements, the local environment and the criteria for the stability of the riverway, the 22.0×1040 m^2 clearance is selected in respect to the lower and upper water levels of the river.

For the computational purpose, each main pylon incorporates 48 stay-cables, 24 on either side, with each cable consisting of A416 parallel strands installed inside a coating duct.

Modelization of the Tower

Since one of the objectives of this work is to describe and to assess the controllability of a bridge tower but not to give an exact understanding of its structural characteristics, an evaluation of structural properties of the tower is given according to the well known linear theory of finite element analysis. The two legs and the connection of each tower are replaced by one simple column in two-dimensional analysis. The height of the tower is 258.98 m measured from the base level to the top saddle. The two main cables are 34m distant from one another and are accommodated by four saddles located at the top of the tower legs. The tower legs and cross-beams are PC structure. The stiffening girder is made of PC box section in the side span and steel box in the middle spans section, respectively. The centre-lines of the tower legs are 50m distant from one another at the bas level. This distance is reduced to 34m at the top. The width of the leg is constant 6 m in the tower plane, while it tapers in the in-plane of the bridge from 16 m at the base level to 8 m at the top. The structure is subdivided into finite elements or members of different sectional properties. Each member has two nodal points. There are three degrees of freedom at each node making a total of six degrees if freedom per element u_1, v_1, θ_1, u_2, v_2, θ_2. Since the general stiffness and mass matrices of the system can be easily assembled, the general damping matrix of the system is computed by the extended Rayleigh method.

Control strategy: Active Tendon Control

A lot of researches and developments of active and/or semi-active dampers have been carried out during the past several years because of the high performance and low power demand behind involved actuators [12, 13, 7]. The semi-active hydraulic actuator concept is attractive because it provides enhanced vibration suppression without requiring excessive external power. Figure 3 shows actuator locations on the column as it is adopted in the present work. When an *n*-DOF discrete-parameter structure is subjected to environmental loads *w*(t)

and counteracted by control forces F(t), its governing equations can be written in matrix form as:

$$M\ddot{u}(t) + C\dot{u}(t) + Ku(t) = BF(t) + Ew(t) \quad (1)$$

where: $u(t)$ is the $n\times1$ displacement vector; $\boldsymbol{M}$, $\boldsymbol{C}$ and $\boldsymbol{K}$ are respectively, the $n\times n$ mass, damping and stiffness matrices; **E** is the $n\times l$ location matrix of the excitation loads; $\boldsymbol{B}$ is the $n\times q$ location matrix of the control force; $F(t)$ is the $q\times1$ control force vector with characteristics satisfying the control strategy; and $w(t)$ is $l\times1$ matrix representing various directions of the excitation loads.

A modern structural control may have many inputs and outputs, and they may be interrelated in a complicated manner. The state space methods for analysis of control systems are best suited to deal with several interrelated input-response systems that are required to be optimized, and the state variable is thus expressed as $z(t) = [u(t),u(t)]^T$. The analytical solution of Equation 1, transformed into the state space form, was expressed in discrete form by the same author [14]. Current required active control forces are found by minimizing the quadratic objective index (or cost function)

$$J(k) = z^T(k)Qz(k) + u^T(k)Ru(k) \quad (2)$$

where: Q is the $2n\times2n$ symmetric positive semi-definite weighting matrix for the responses; R is the $q\times q$ symmetric positive definite weighting matrix for the input control forces.

Discrete-time Control by Linearization of the Feedback Gain

To develop an optimal solution, it is necessary to create a cost function that includes the appropriately chosen weighted variables such as the state vector $z(t)$ and the applied control forces $F(t)$. An optimal solution is defined by minimizing this cost function with respect to the control, and the state and being constrained by the appropriate equation of motion. It is required to create a continuous quadratic function J, which will be minimized by appropriate control gain G subjected to the equation of motion. A clear understanding of the gain matrix with respect to displacement and the velocity components shows that they have different weight or amount of contribution on the control gain. It is possible to reformulate the gain matrix by simply decomposing its displacement and velocity components and then multiplying each one by a certain proportionality coefficient related to the desired expectations. Taking the components of G linearly related to the displacement and to the velocity, one can easily formulate it as G_L :

$$G_L = G_1 + G_2 = \alpha_1 G_d + \alpha_2 G_v \tag{3}$$

where G_d and G_v are respectively displacement and velocity gain matrices with the order of G.

Using Equation (1) in the state space form and defining the quadratic cost function J in term of the gain matrix given in Equation (3) lead to the minimization of the linearized augmented cost function J_L with respect to the partial gain matrices G_1 and G_2 or to the linearized Gain G_L.

$$\begin{aligned} J_L = \sum_{k=0}^{n} [&z^T(k) Q_L z(k) + 2 z^T(k) G_1^T R G_2 z(k) + \\ &\lambda^T(k)\left(\overline{A}_L z(k) + \overline{E} w(k) - \dot{z}(k+1)\right)] \end{aligned} \tag{4}$$

The necessary conditions for optimality are obtained by imposing the first variational of the discrete augmented cost function J_L with respect to the control and the state equal to zero[15]. The form of these generated equations encourages the use of a gradient search to obtain numerical results for minimizing J_L:

$$\frac{\partial J_L}{\partial G_L} = \frac{\partial J_L}{\partial G_2} = \frac{\partial J_L}{\partial G_1} \tag{5}$$

These two last equations are the same in nature with the one obtained in general optimal control, and lead to the general form that justifies the use of the gain in Equation (3) without disturbing the stability of control system. The state equations for *z(k)* are shown to be independent of the Lagrange multipliers or co-state vectors $\lambda(k) = [\lambda_1(k), \lambda_2(k)]^T$, but they contain the state variables explicitly. Therefore, it is possible to solve the state equations forward in time first and then solve the co-state equations backward to obtain the complete time histories for both. Thus, it is possible to find *G* with any well known classical method and then linearize it with one of the coefficients among α_1 or α_2 greater than the one affected to the gain component with more response reduction. The other coefficient less than unity will then be affected to the component with less response reduction.

For linear optimal shift-invariant state feedback control, the co-state vector $\lambda(k)$ has the form $\lambda(k) = Pz(k)$, with P being a $2n \times 2n$ constant matrix. Hence the control force vector is linearly related to the state variables of future time step as

$$u(k) = -(2R + \overline{B}^T P \overline{B})^{-1} \overline{B}^T P \overline{A} z(k) \tag{6}$$

Based on the equations the unknown matrix P can be determined by solving the following Riccati matrix equation

$$P = \overline{A}^T P \overline{A} + 2Q - \overline{A}^T P \overline{B}\left(2R + \overline{B}^T P \overline{B}\right)^{-1} \overline{B}^T P \overline{A} \tag{7}$$

Time Delay Compensation

The discrete-time control system described by the linearization procedure is idealized when the control forces $u(k)$ at step k has been computed with the known state response of $z(k\text{-}1)$ and $z(k\text{-}2)$ at the time step $(k\text{-}1)$. In practice, time has to be consumed during data processing, online computation and control force application. Inevitable time delay in control execution makes it necessary to consider appropriate modifications to the control algorithm. In the presence of time delay $m\Delta t$, the state equation becomes

$$z(k) = A_0 z(k-1) + B_0 u(k-m-1) + B_1 u(k-m) + E_0 w(k-1) + E_1 w(k) \quad (8)$$

where: m is the number of delayed time steps; A_0 is the discrete time system matrix; B_0 and B_1 are the control force matrices at the previous and current steps; E_0 and E_1 are the excitation force matrices at the previous and current steps. The application of the control force $u(k)$ is out of phase with the state variables $z(k)$ by $-m\Delta t$. With time-delay, the discrete performance in Equation (2) in discrete form can be rewritten as

$$J(k) = \sum_{k=0}^{n} z^T(k) Q z(k) + u^T(k-m) R u(k-m) \quad (9)$$

Considering time-delay the optimization problem is converted again to the minimization of this performance index subjected to the constraint of Equation (6) and one can find that the time-delay control forces $u(k\text{-}m)$ are also linearly related to the current state variables $z(k)$ by

$$u(k-m) = G_L z(k) \quad (10)$$

The control law represented by this last equation cannot be implemented since the control forces $u(k\text{-}m)$ at step $(k\text{-}m)$ depend on the state variables $z(k)$ that is expected to be known m steps ahead. After substituting Equation (10) into the state Equation (8) without considering the excitation load $w(k)$, the current state variables $z(k)$ and the previous state variables $z(k\text{-}1)$ are related by $z(k)=Tz(k\text{-}1)$. With the RICATI matrix equation P known, the $2n \times 2n$ transition matrix T is defined by:

$$\begin{aligned} T &= \left(I + \frac{1}{2} B_1 R^{-1} \overline{B}^T P \right)^{-1} \left(A_0 - \frac{1}{2} B_0 R^{-1} \overline{B}^T P \right) \\ &= \left(I - B_1 G_L \right)^{-1} \left(A_0 + B_0 G_L \right) \end{aligned} \quad (11)$$

By applying this last equation continuously to Equation (10), the time-delay control force $u(k\text{-}m)$ can be generated from the time-delay state variables $z(k\text{-}m)$ as

$$u(k-m) = G_L T^m z(k-m) = G_D z(k-m) \quad (12)$$

where $G_D=G_L T^m$ is the time-delay feedback gain matrix with the same order of matrices G and G_L.

The dynamic equation of the present discrete-time system in the presence of time-delay remains simply a difference equation as before and the stability problem associated with this procedure can be easily transformed to an eigenvalue problem of the augmented associated effective system matrix defined in Equation (4). The control strategy behind this method requires that the system be controlled every time when its monitored response crosses a threshold in a particular location, and that the amplitudes of the control forces furnished by the actuators be chosen so as to minimize the given cost function with the bounded coefficients.

Results and Discussions

Two numerical examples, a sinusoidal ground motion and a seismic excitation of the proposed structural model, are presented to verify the feasibility of the proposed control algorithms. In the present analysis the following expressions are referred to:

- X_0= horizontal displacement history of the top-tower without control;
- *SF* = horizontal displacement history of the top-tower with *state-feedback* control;
- *DF* = horizontal displacement history of top-tower with *displacement-feedback* control;
- *VF* = horizontal displacement history of top-tower with *velocity-feedback* control;
- SF_t = horizontal displacement of top-tower with *state-feedback* and *time-delay;*
- DF_t = horizontal displacement of tower with *displacement-feedback* and *time-delay;*
- $X_{tp}(t)$ = horizontal displacement of top-tower;
- $Y_{ms}(t)$ = vertical displacement of the middle span section at time t;
- Y_0 = vertical maximal displacement of the middle span section *without control;*
- X_c = horizontal maximal top-tower displacement of the *state-feedback* case;
- X_{cd} = horizontal maximal top-tower displacement of the *displacement-feedback* case;
- X_{cv} = horizontal maximal top-tower displacement of the *velocity-feedback* case;
- X_{ct} = maximal top-tower horizontal displacement with *SF* and *time delay;*
- X_{cdt} = maximal top-tower horizontal displacement with *DF* and *time delay*

- α_1/α_2 = the linearization proportionality coefficients;
- Cf = maximal control force applied at top-tower.
- m = number of steps in time delay;
- β = control effectiveness and economy coefficient.

Responses Simulation under Sinusoidal Excitation

Let us consider the horizontal and vertical motions of the model subjected to sinusoidal base acceleration $\ddot{x}_0(k)$. As shown in Figure 3, the control force is applied to the top-tower trough a set of tendons connected to an actuator placed at the top or at the ground level. From the 2-dimension model shown earlier, the sinusoidal ground acceleration in both x-x and y-y direction is expressed as $w(k)=0.4g\times\sin(0.8w_0k\Delta t)$, where g is the gravitation constant and w_0 the seventh circular frequency of the structure. The seventh mode is chosen at this stage since it is the lowest mode that affects the top-tower horizontal displacement. This frequency is pre-multiplied by 0.8 only to assess the control effect on the increased-near-to-resonance structural response. The structural stiffness, mass and damping matrices as well as other variables have been explained earlier.

Discrete-time Control by the Linearization of Feedback Gain

The minimization procedure obtained by minimizing Equation (2) only may not always give the best result with the commercial software package for any structural model, as shown in Table 1 with α_1/α_2 = 1.0/1.0 and β =1, since there is no significant difference between controlled and uncontrolled cases. Further increase of the control effectiveness coefficient β up to 0.01 shows that there is instability with the velocity feedback control procedure, since its maximal controlled response X_{cv} is almost the double of the non-controlled one X_0. In the same time, we notice a slight reduction of the pick response for the displacement feedback control case X_{cd}. And since there is a greater influence of instability generated by the velocity feedback control on the general response, the state feedback controlled response X_c is also greater than the non-controlled case. Solving this velocity-instability and displacement-gain optimization is the justification of the use of the linearization of the gain matrix G.

The results obtained from the linearized feedback gain matrix G_L are shown also in Table 1 for four pairs of the linearization coefficients α_1/α_2 with a fixed value of β =0.01. We

can see that the instability due to the velocity feedback is reduced by giving a stable response near to the non-controlled case, while the state and the displacement feedback responses can be reduced significantly to a near-to-zero position if the imposed linearization proportionality coefficient α_1 is further increased. For the present structure and for those with noticeable computational irregularities such as instability, modelling errors, spill over and so on, the linearization procedure appears to be adequate for it intends to reduce undesirable responses while activating needed ones.

Table 1. Maximal displacements for a sinusoidal excitation after the Linearization.

Maximal Values	α_1 / α_2					
	1.0/1.0		3.9 / 0.1	9.9 / 0.1	49.9 / 0.1	99.9 / 0.1
	β = 1.0	β = 0.01	β =0.01			
X_0, (m)	5.93	5.93	5.93	5.93	5.93	5.93
X_c, (m)	5.92	11.4	4.44	3.18	1.37	0.66
X_{cd}, (m)	5.93	5.44	4.39	3.14	1.12	0.65
X_{cv}, (m)	5.93	12.4	5.97	5.97	5.97	5.97

Time Delay Compensation

The Dynamic characteristics of the structural model can be easily studied by evaluating the eigenvalues of the effective system stiffness matrix of Equation (2) for different case of time delay *m*. It can be seen that with inclusion of the transition matrix T^m from Equation (12), the natural frequencies are greatly changed and the system equivalent damping are also increased. In frequency-domain, the effectiveness of the time-delay compensation will be obvious since the pick amplitude will be greatly influenced in the considered mode with and without compensation. Frequency analysis is not performed here to verify the question for this is not the key problem to be tackled in this work.

The results in time-domain show the importance of time-delay compensation. When *m*=5, the time-delay is 10 ms and the system can still operate safely without instability, but the compensation effect is noticeable on the maximal horizontal displacement amplitude of the top-pier. This situation remains without great change up to *m*=13 with time-delay 26 ms as shown in Table 2 and Figure 4. Further increase in time-delay displays an abrupt instability of structural responses in the case without compensation. When time-delay compensation is considered, the control system remains stable for *m*= 14 and *m*=15. During instability, the

corresponding amplitude-change increases as a function of time delay and the relative displacements are growing faster as time increases.

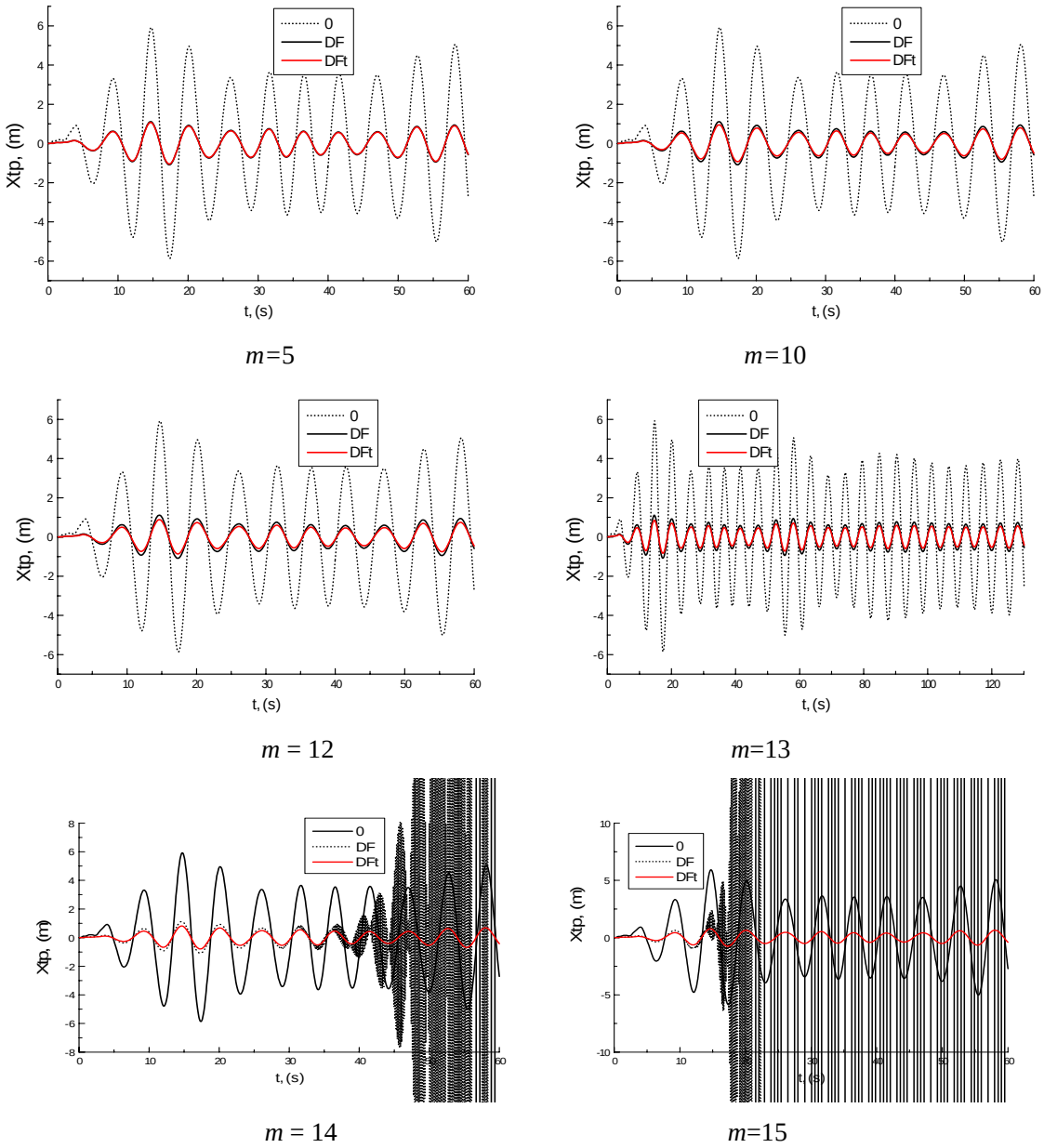

***Figure 4**. Top-tower relative displacement under a sinusoidal excitation with time-delay consideration for the displacement feedback (α= 49.9/0.1; β =0.01).*

Table 2. Maximal displacements with time delay consideration (α_1 / α_2 = 49.9/0.1; β=0.01)

Maximal Values	Time delay *m*					
	5	10	12	13	14	15
Xo (m)	5.93	5.93	5.93	5.93	5.93	5.93
Xcd (m)	1.15	1.12	1.12	1.12	***75.4***	***1.8E+17***
Xcdt (m)	1.07	0.95	0.89	0.85	0.81	0.77

Responses Simulation under Earthquake

The effectiveness of the developed theory is again determined by studying the responses of the system under the Elcentro earthquake input (Imperial Valley 1940). The horizontal component (S00E with PGA = 0.3417g) and the vertical component (PGA = 0.2063g) of the earthquake are simultaneously applied to the system without taking into account the time-difference input between considered support motions. Therefore the time-difference between the arrivals of the input at the two towers is negligible compared to the considered time-delay in the present work. The reason for choosing such input is that it represents a benchmark with which one can easily compare the results obtained by the present formulation. Structural properties of the model remain unchanged as well as the control weighting matrices. Since all the earthquake records are discrete, the discrete-time formulation developed earlier and followed by sinusoidal numerical analysis is suitable to be used at this stage without any discrepancy. First, horizontal (X) and vertical (Y) excitations are separately applied to the model structure. The calculated results are shown in Figure 5.

Shown in Table 3 are the Maximal displacements $X(t)$ and $Y(t)$ by the Linearization of the Feedback Gain under El-Centro input with α_1 / α_2 =49.9/0.1 and β =0.01. The results show almost 83 % reduction of the top-tower horizontal displacements for the state (SF) and the displacement (DF) feedback controls. This reduction is limited only to 75 % for a dual horizontal and vertical excitations applied at the same time. This situation was expected since the influence of both inputs, even different in modal components, is less consistent in term of negative input energy to the structure.

Table 3. Maximal displacements $X(t)$ and $Y(t)$ by the Linearization of the Feedback Gain under El-Centro input with α_1 / α_2 =49.9/0.1 and β =0.01.

Maximal Values (m)	Horizontal component		Vertical component		Horizontal & vertical	
	Top-tower	Mid-span	Top-tower	Mid-span	Top-tower	Mid-span
X_0 / Y_0	0.22	0.49	0.39	13.6	0.36	12.7
X_c / Y_c	0.04	0.48	0.08	13.1	0.09	12.6
X_{cd} / Y_{cd}	0.04	0.47	0.08	12.5	0.08	11.8
X_{cv} / Y_{cv}	0.23	0.49	0.40	13.8	0.40	12.9

As was noted in previous works done by the authors [8], the top-tower displacement control procedure gives little influence on the middle-span vertical displacement. From a

closer look of the middle span displacement history, it is seen that vertical responses due to horizontal excitations (*X*) are damped by the structural damping, while middle-span vertical responses due to vertical (*Y*-*Y*) or dual (*X*-*Y*) excitations are almost stable after reaching their maximal values.

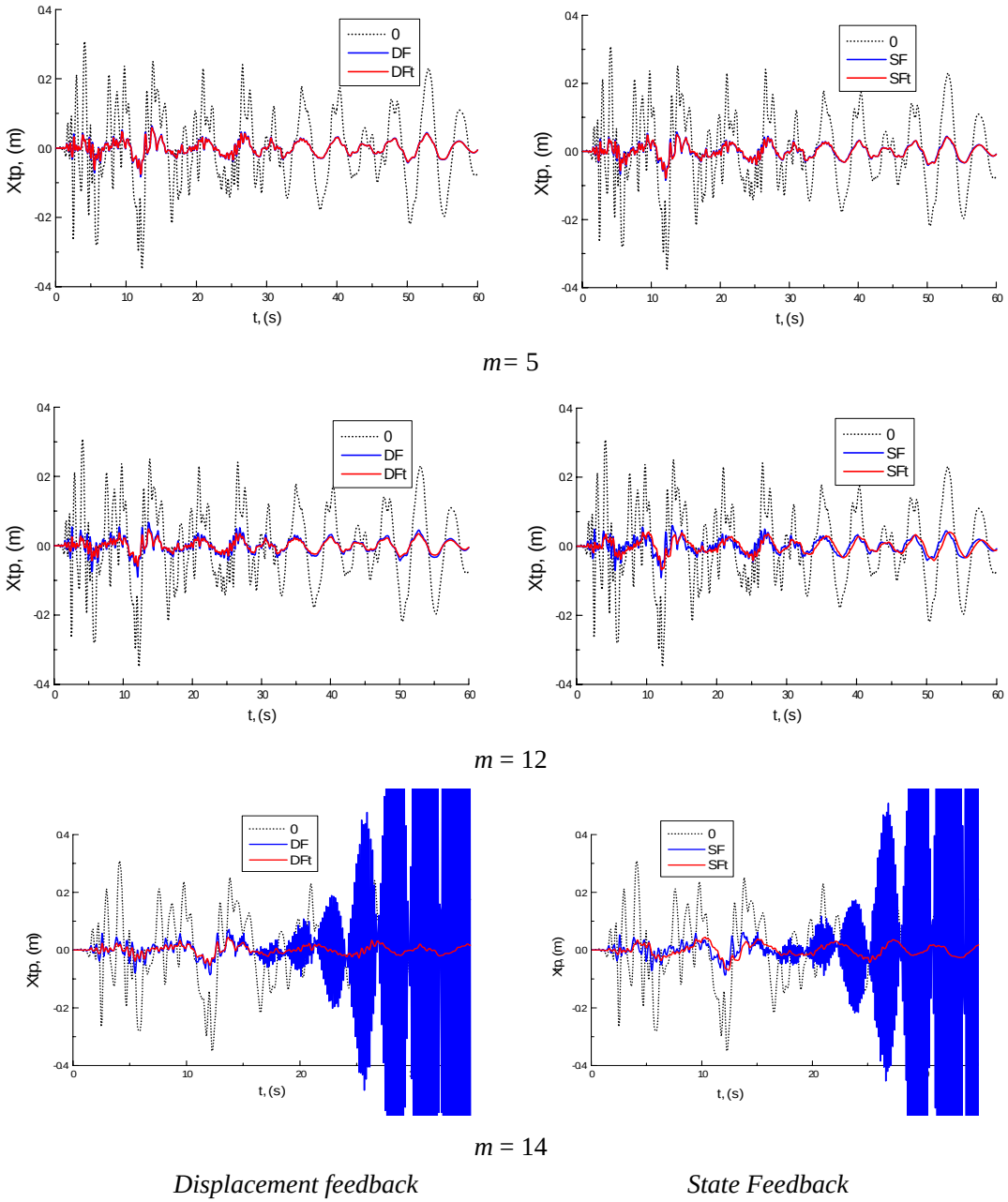

Figure 5. *Top-tower horizontal displacements under El-Centro excitation without and with time-delay compensation for the state and the displacement feedback (X-Y). (α= 49.9/0.1 & β =0.01).*

The shape without or with control of the first two diagrams of the top-tower response is first similar to the process of a single DOF damped structure in resonance. And then, when the effect of the excitation load vanishes, the shape is similar to a free vibration damping process that may need a relatively long time before its consumption. This allows us to conclude that the control of horizontal displacements of the present tower has little effect on the vertical responses of the middle span structure as seen in Table 4.

Taking into account time-delay effect for Elcentro earthquake, Figure 5 displays almost the same conclusions that have been made with the sinusoidal input in Figure 3. For both state and displacement feedback controls, the rise of the response amplitude first is weak proportional to the time-delay *m*. Therefore, when *m* reaches 14, this weak proportionality is destroyed and replaced by a strong instability if no control measure is taken, as shown also in Table 4. It is evident that the Linearization of the Feedback Gain method can be successfully applied to earthquake inputs with practical considerations such as discrete time control, time-delay, and other control algorithms.

Table 4. Maximal displacements with time delay consideration under El-Centro input. (α_1 / α_2 =49.9/0.1; β=0.01)

Maximal Values (m)	Time delay *m*					
	State Feedback			Displacement Feedback		
	05	12	14	05	12	14
X_0	0.36	0.36	0.36	0.36	0.36	0.36
X_c / X_{cd}	0.09	0.09	∞	0.09	0.10	∞
X_{ct} / X_{cdt}	0.08	0.07	0.07	0.08	0.06	0.05

Concluding Remarks

The following conclusions can be drawn from the study:

- The present method is efficient. The controlled horizontal displacements obtained from the state and the displacement feedback cases are substantially reduced from 5.93m to 0.65m corresponding to 90% reduction. The present algorithm allows the user to obtain full vibration suppression if the imposed linearization proportionality coefficient α_1 is increased and if control mechanisms are available.
- A feedback compensation scheme to tackle time-delay effects is realized by simply modifying the linearized feedback gain matrix of the ideal control system. If time-delay is

neglected, the control system is susceptible to develop dynamic instability. Therefore it is better not to apply control actions into a structural system only after the time-delay is analyzed and tackled properly.

- Although the case study in this work is for a reduced order model with only 46 nodes and 71 elements, the proposed discrete-time control method can be actually applied to real structures with unlimited DOFs in plane as well as in space.
- During simulations, structural properties were assumed invariant with time, but during severe earthquakes some (if not most) elements often work in elasto-plastic or plastic stage and the present control algorithm in that case is inadequate. A parallel work is being done to consider the variation of the linearized gain matrix as a known or unknown function of the change in structural properties of the model during exploitation. This approach is still under consideration since the gain matrix (different at each time step) will rather be deduced at a certain extent from known conditions.
- The efficiency of a tendon control in high-rise structures must be subjected to justification since the self-mass of the control cable will increase the system mass and therefore lower the frequency range of the system. Depending on the distance to span and on the height of the tower, what should the control cable optimal diameter be to ameliorate the system's structural characteristics? In which way will it be structurally fit and mechanically efficient to use the main suspension cable as a control cable? The thought of these possibilities and eventual answers are to be justified further.

Acknowledgements

This project was sponsored by the by the National Natural Science Foundation of China (Grant N° 90715008), the Flander (Belgium-China) Bilateral Project (BIL07/07) and the National Civil Engineering Laboratory (LABOGENIE) of Cameroon.

References

1 Mohamed Abdel-Rohman, and A. H. Nayfeh, *Active Control of Nonlinear Oscillations in Bridges*, ASCE Journal of Engineering Mechanics, 1987, Vol. 113 N°3, p. 335-348.

2 Deger Y., R. Cantieni, de Smet, C.A.M. Felber, *Finite Element Model Optimization of the New Rhine Bridge based on Ambient Vibration Testing,* Proceeding of the Third European

Conference on Structural Dynamic, EURODYN-6-96, Roterdam, June 1996, Vol.2, p. 817-822.

3 Achkire Y. and A. Premont, *Active Tendon Control of Cable Stayed Bridges*, Earthquake Engineering and Structural Dynamics, 1996, Vol. 25 p. 585-597.

4 Hiroshi Kobayashi, Masao Hosomi, and Kazuyoshi Koba, *Tendon Control for Cable Stayed Bridge Vibration*. First World Conference on Structural Control, Los Angeles California USA, 1994, Vol. 3(FA1); p. 23-29.

5 Pennung Warnitchai, Yozo Fujino, D. M. Pacheco and R. Agret, *An Experimental Study on Active Tendon Control of Cable-Stayed Bridges*, Earthquake Engineering and Structural Dynamics, 1993, Vol.22, p. 93-111.

6 Bernd Köberl, Johann Kollegger. *High Frequency Test Facility for Stay Cables and Tendons*, Structural Engineering International, 2008, SEI Vol.18, N° 3, p 259-264.

7 Akong Charles Ntika , *Power Privatisation in Cameroon, the Chad Oil Pipeline and Skewed Development*. Pambazuka News, Issue 144, February 2004. http://pambazuka.org/en/category/comment/20260

8 Minsili, L. S., He Xia, L. M. Ayina Ohandja, M. Mpele. *An active Vibration Control Method of Bridge Structures by the Linearization of Feedback Gain Matrix*. Botswana Journal of Technology, Vol. 18 N° 1. p. 1-9, April 2009.

9 Niels J. Gimsing, *Cable Supported Bridges : Concept and Design*, Copyright by John Wiley & Sons Ltd, England, 1997, p. 5-85.

10 Xiao Ru Cheng, Loxi Heng, *Design Research of a Combined Cable Supported Bridge on the Eastside of the Inner Ling-Ding Island*, The Thirteen Academic Conference on Chinese Bridges, ShangHai-China, November 1998, p.79-86.

11 ECTA-BTP / SCETAUROUTE Int. / SCET-Cameroun, *Rehabilitation du Pont sur le Wouri: Avant Projet Détaillé, Etude du Renforcement*, Financement AFD, Communauté Urbaine de Douala, Cameroon, 2004.

12 Patten W. N., R. L. Sack, W. Yen, C. Mo and H. C. Wu, *Controlled semi-active hydraulic vibration absorber for bridges,* Journal of Structural Engineering, 1994,Vol. 122(2), pp. 187-192.

13 Kurata N., Kobory T, Takahashi M, Niwa N, and Midorikawa H, *Actual Seismic Responses of Controlled Building with Semi-Active Damper System*. Earthquake Engineering and Structural Dynamics, 1999, Vol.28, p. 1427-1447.

14 Minsili L. S., Zhong Tieyi et He Xia, *A Passive Vibration Control Method for Truss Bridge Structures using Friction Dampers*, The six International symposium on structural engineering for young experts ISSEYE-6, Kunming China, August 2000, p. 385-394.

15 Kabamba P.T. and R. W. Longman, *An Integrated Approach to Reduced Order Control Theory*, Optimal Control Applications and Methods, 1983, Vol. 4, p.405-415.